Journal of Control, Automation and Electrical Systems (2019) 30:802–811
https://doi.org/10.1007/s40313-019-00478-7

An Interval Arithmetic-Based Power Flow Algorithm for Radial Distribution Network with Distributed Generation

Helton do Nascimento Alves[1]

Received: 12 February 2019 / Revised: 14 May 2019 / Accepted: 21 May 2019 / Published online: 29 May 2019

Abstract
This paper presents a primary distribution system power flow analysis in the presence of uncertainties in distributed generation and loads. The algorithm is based on a backward/forward sweep power flow algorithm with power flow updates. The uncertainties are modelled by real compact intervals based on interval arithmetic. A simple and interactive method is used to consider the generator bus voltage controls and reactive power limits. Simulations are presented on a 69-bus, a 104-bus and a 282-bus test distribution system to verify the effectiveness of the proposed method. The power flow solution bounds obtained by the proposed algorithm are compared to those calculated using a Monte Carlo simulation. The results confirm the efficiency of the proposed method which makes it promising to solve real problems of power flow analysis in distribution feeders.

Keywords Backward/forward power summation method · Distributed generation · Distribution networks · Interval arithmetic · Uncertainties

1 Introduction

Recently, a remarkable role has been played by distributed power generation (DGs) in distribution network. DGs are directly connected to the distribution system, and they are important variables in power system planning and operation. DGs are usually sources with uncertainty, because they depend on unpredictable energy resources such as wind, sunlight and water flow. These uncertainties added with uncertain loads are important factors that should be taken into account in distribution system power flow analysis (Hadjsaid et al. 1999; Alvarado et al. 1992; Vaccaro and Villacci 2009).

A classical power system load flow is based on deterministic data, and several assumptions are made to model the power system. Thus, only a specific operation point is provided by the load flow solution. More realistic solutions are provided by the load flow as the uncertainties of data are considered (Li 2005). Many methodologies have been proposed in the literature for solving load flows considering uncertainties. These methodologies can usually be classified into three categories: probabilistic modelling (Borkowska 1974; Su 2005), fuzzy set theory modelling (Kenarangui and Seifi 1994; Bijwe et al. 2005) and interval arithmetic modelling (Pereira et al. 2012; Zhang et al. 2017). The interval arithmetic represents measurements errors or uncertain data through a range of possibilities, being a simple way to treat the uncertainties inherent in the electric energy systems.

In the literature, several works have developed interval power flows for transmission application (Alvarado et al. 1992; Vaccaro et al. 2010; Pereira et al. 2012; Zhang et al. 2017; Liao et al. 2017) and for distribution networks application (Das 2002, 2014; Gu et al. 2014; Luo et al. 2017; Wang et al. 2018). In special, backward/forward current summation (BFCS) algorithm is applied for interval distribution power flow (Das 2002, 2014; Gu et al. 2014; Luo et al. 2017). In the literature review made in this paper, no one interval distribution power flow based on backward/forward power summation method (BFPS) was identified. In relation to DGs' intermittent, Luo et al. (2017) considered the uncertainties in loads and in DGs units modelled as PQ-node. Das (2014) considered the uncertainties of the active power produced by a wind turbine generating system. In both papers, the presence of DG units modelled as PV-node was not considered.

✉ Helton do Nascimento Alves
helton@ifma.edu.br

1 Department of Electrical Engineering, Instituto Federal do Maranhão (IFMA), São Luís, MA 65030-000, Brazil

Due to the differences that exist between the BFCS and the BFPS calculation process, the quantity and type of interval arithmetic operations when applied in their process are also different. In this case, the conservatism inherent in all interval arithmetic computations will have different effects in each algorithm. Besides, the interval bus voltages in polar form (magnitude and angle) provided by interval arithmetic BFPS and the interval bus voltages in rectangular form (real and imaginary) provided by interval arithmetic BFCS do not have the same direct association as polar and rectangular numbers have in complex arithmetic. In interval arithmetic backward/forward current summation (IABFCS), the interval voltages in polar form (magnitude and angle) are calculated from their respective complex interval voltages. In this case, it is supposed that the lower and upper bounds of complex values define the lower and upper bounds of magnitude and angle values, respectively. That assumption includes more errors in estimating the polar interval voltage values. Considering that polar coordinate voltages along the distribution network are usually more important information for power system planning and operation than the rectangular coordinate voltages, their accuracy is very important. On the other hand, if backward/forward power summation (BFPS) method is applied for interval distribution power flow, the polar interval voltages are directly calculated and no assumptions about their bounds are needed. Besides, the voltage control demanded by PV-node DGs is easier to handle in BFPS than BFCS, because the bus voltages magnitude is calculated directly in BFPS process.

In this paper, an interval arithmetic-based power flow algorithm using backward/forward power summation method is proposed (IABFPS). The main contributions of this paper are as follows:

- Uncertainties in DGs as well as in loads are considered.
- DGs units modelled as PV-node are considered.
- A simple model for PV-node DG is used.
- Different from the interval arithmetic backward/forward sweep power flow analysis algorithms presented in the literature, IABFPS is based on power summation, instead current summation.
- IABFPS provides polar interval voltage values more accurate than IABFCS.
- The accuracies of IABFPS and Monte Carlo simulation algorithm (MCS) are quite comparable.
- The proposed approach demonstrates to be effective in accommodating the uncertainties of DGs and loads, and it has low CPU time, being appropriate for online applications.

2 Problem Formulation

2.1 Interval Arithmetic

Interval arithmetic represents unknown values, rounding error, inaccurate data, approximations and truncation errors by boundary real numbers in numerical computation. An interval number $[\underline{x}, \bar{x}]$ is the set of real numbers x such that $\left\{x \in \Re | \underline{x} \leq x \leq \bar{x}\right\}$ where $\underline{x}$ and $\bar{x}$ are defined as the lower and upper limits of the range, respectively. Let $X = \left[\underline{x}, \bar{x}\right]$ and $Y = \left[\underline{y}, \bar{y}\right]$ be two interval numbers, the elementary interval arithmetic operation is given as:

$$X + Y = \left[\underline{x} + \underline{y}, \bar{x} + \bar{y}\right] \tag{1}$$

$$X - Y = \left[\underline{x} - \bar{y}, \bar{x} - \underline{y}\right] \tag{2}$$

$$\begin{aligned} X * Y = \Big[&\min\left(\underline{x} * \underline{y}, \underline{x} * \bar{y}, \bar{x} * \underline{y}, \bar{x} * \bar{y}\right), \\ &\max\left(\underline{x} * \underline{y}, \underline{x} * \bar{y}, \bar{x} * \underline{y}, \bar{x} * \bar{y}\right)\Big] \end{aligned} \tag{3}$$

$$X \div Y = X * \left[1/\bar{y},\ 1/\underline{y}\right], \quad \text{if} \quad 0 \notin= \left[\underline{y}, \bar{y}\right] \tag{4}$$

$$\text{Distance } (X, Y) = \max\left(\left|\underline{x} - \underline{y}\right|, |\bar{x} - \bar{y}|\right) \tag{5}$$

2.2 Interval Model for PV-Bus DG

Including PV-node DGs in BFPS demands the calculation of the reactive powers that they must inject in the power system to maintain the PV-node voltages magnitude in specified values. The solution can be found through an optimization process or an iterative process. In both cases, the error between the measured voltage and the specified voltage in PV-node DG units is the object function that must be minimized. The algorithm needs to include the reactive and voltage limits constraints for each generator. If reactive power limits are violated, the PV-node DG is converted into a PQ-node DG with the reactive power set at the limiting value.

In this paper, PV-node DG is included in IABFPS through the compensation method proposed by Cheng and Shirmohammadi (1995). Due to the uncertainties in loads demand and DG generation, in this work it is assumed that the specified voltage for the PV-nodes may have a small variation of up to 2% of the specified voltage value (named interval PV-node voltage). The steps shown below illustrate the compensation method applied in IABFPS.

1. Interval PV-node voltage magnitude is defined for every PV-node DG.
2. PV-node sensitivity matrix Z_{PV} is calculated according to Eq. 6.
3. Polar interval voltage values are calculated by IABFPS considering the interval active power of PV-node DGs.
4. The interval reactive power of PV-node DGs obtained in step 3 is corrected based on Z_{PV} and interval PV-node voltage mismatch (Eq. 7).
5. If interval PV-node voltage mismatch is less than the voltage convergence criterion, finish the process, otherwise go to step 3 using the new interval reactive power injection of PV-node DGs calculated in step 4.

The dimension of Z_{PV} is equal to the number of PV-node DGs. Considering a distribution network with $j = 1,\ldots,k$ PV-node DGs, PV-node sensitivity matrix (Z_{PV}) is given as,

$$Z_{\mathrm{PV}} = \begin{vmatrix} V_{11} & V_{12} & \cdots & V_{1k} \\ V_{21} & \ddots & \vdots & V_{2k} \\ \vdots & \ldots & \ddots & \vdots \\ V_{k1} & V_{k2} & \ldots & V_{kk} \end{vmatrix} \tag{6}$$

where V_{jj} is the voltage in PV-node j and V_{jp} is the voltage in PV-node p determined by one back and forward sweep as injecting the current $I_j = 0 + 1i$ to PV-node j with all loads and sources removed.

Interval reactive power injection of PV-node j corrected by compensation method is calculated as,

$$Q_j^N = Q_j^O + |X_{\mathrm{PV}}|^{-1} \Delta V_j \tag{7}$$

where Q_j^O is interval reactive power injection in PV-node j obtained by IABFPS, Q_j^N is interval reactive power injection in PV-node j corrected by compensation method, X_{PV} is the reactance of Z_{PV} and ΔV_j is the interval PV-node voltage mismatch between the interval voltage calculated by IABFPS (V_j^O) in PV-node j and its interval PV-node voltage (V_j^{PV}).

3 Proposed Algorithm

In order to analyse the primary distribution system power flow in the presence of uncertainties associated with load demands and intermittent generation sources, an interval arithmetic-based power flow algorithm using backward/forward power summation method is proposed. The IABFPS uses the basic backward/forward power summation method power flow presented in Das et al. (1994), but to account for the uncertainty of load demands and output power of DGs, the real and reactive power have been treated as interval number and the real arithmetic has been replaced by real interval arithmetic.

Since interval arithmetic was applied in power flow analysis (Alvarado et al. 1992), some strategies have been adopted to reduce the conservatism inherent in all interval arithmetic computations. In IABFPS, the nonlinear equations present in the load flow analysis are solved in an iterative process, without linearization of power flow equations and without calculation of the inverse matrix. Those features are important in reducing the conservatism present in interval arithmetic.

In order to transform loads demand and output power of DGs into interval forms, the loading pattern of the distribution network and nominal output power of DGs are taken as reference. Load/generation uncertainties have been taken into account by assuming that they vary over a certain range. It is assumed that uncertainties considered in DGs are achievable. In this paper, for convenience, the lower and upper bound values of interval numbers are assumed to have the reference values as their arithmetic mean. However, it is very simple to adjust the proposed algorithm to have different associations among reference values and minimum and maximum values of interval numbers. It is assigned uncertainty tolerances for load demands, output active and reactive power of PQ-node DGs and output active power of PV-node DGs.

The load uncertainties in bus k is assumed as,

$$\mathrm{PIL}_k = [\mathrm{PL}_k(1 - u_{\mathrm{PL}}/100), \mathrm{PL}_k(1 + u_{\mathrm{PL}}/100)] \tag{8}$$

$$\mathrm{QIL}_k = \left[\mathrm{QL}_k\left(1 - u_{\mathrm{QL}}/100\right), \mathrm{QL}_k\left(1 + u_{\mathrm{QL}}/100\right)\right] \tag{9}$$

where PIL_k is the interval active power of load demand in bus k; QIL_k is the interval reactive power of load demand in bus k; PL_k is the reference active power of load in bus k; QL_k is the reference reactive power of load in bus k; u_{PL} is the uncertainty tolerance for active power of load demand; and u_{QL} is the uncertainty tolerance for reactive power of load demand.

The uncertainties in generated power by PQ-node DG allocated in k are assumed as,

$$\mathrm{PIPQ}_k = \left[\mathrm{PPQ}_k\left(1 - u_{\mathrm{PPQ}}/100\right), \mathrm{PPQ}_k\left(1 + u_{\mathrm{PPQ}}/100\right)\right] \tag{10}$$

$$\mathrm{QIPQ}_k = \left[\mathrm{QPQ}_k\left(1 - u_{\mathrm{QPQ}}/100\right), \mathrm{QPQ}_k\left(1 + u_{\mathrm{QPQ}}/100\right)\right] \tag{11}$$

where PIPQ_k is the interval active power of a PQ-node DG in bus k; QIPQ_k is the interval reactive power of a PQ-node DG in bus k; PPQ_k is the nominal output active power of a PQ-node DG in bus k; QPQ_k is the nominal output reactive power of a PQ-node DG in bus k; u_{PPQ} is the uncertainty tolerance for active power of a PQ-node DG; and u_{QPQ} is the uncertainty tolerance for reactive power of a PQ-node DG.

The uncertainties in generated active power by PV-node DG allocated in k are assumed as:

$$\mathrm{PIPV}_k = [\mathrm{PPV}_k(1 - u_{\mathrm{PPV}}/100), \mathrm{PPV}_k(1 + u_{\mathrm{PPV}}/100)] \tag{12}$$

where PIPV_k is the interval active power of a PV-node DG in bus k; PPV_k is the nominal output active power of a PV-node DG in bus k; and u_{PPV} is the uncertainty tolerance for active power of a PV-node DG.

In the power flow solution, the interval voltage at slack bus is assumed to be the voltage of the root node in both lower and upper bounds. Figure 1 and the steps shown below illustrate the proposed algorithm.

1. Define uncertainty tolerance rate for active power of load demand (u_{PL}), reactive power of load demand (u_{QL}), active power of a PQ-node DG (u_{PPQ}), reactive power of a PQ-node DG (u_{QPQ}) and active power of a PV-node DG (u_{PPV});
2. Based on the original feeder configuration (substation line voltage, impedance of each feeder section, active and reactive power of each load demand and DGs parameters), calculate the interval numbers expressed in Eqs. 8–12;
3. Define a small variation for specified voltage (u_{VPV}) in PV-nodes (up to 2%);
4. Calculate the interval PV-node voltage for each PV-node based on u_{VPV};
5. Calculate the PV-node sensitivity matrix (Eq. 6);
6. Perform IABFPS until the power mismatch from lower and upper boundaries in each node is less than the power convergence criterion. Interval voltage magnitude and angle for all nodes are calculated;
7. Calculate interval PV-node voltage mismatch between the interval voltage calculated by IABFPS in PV-node and its interval PV-node voltage;
8. If lower and upper boundaries of interval PV-nodes voltage mismatches are less than the voltage convergence criterion, finish the process;
9. Calculate the new interval reactive power injection in PV-nodes using Eq. 7 to apply in IABFPS;
10. Go to step 6.

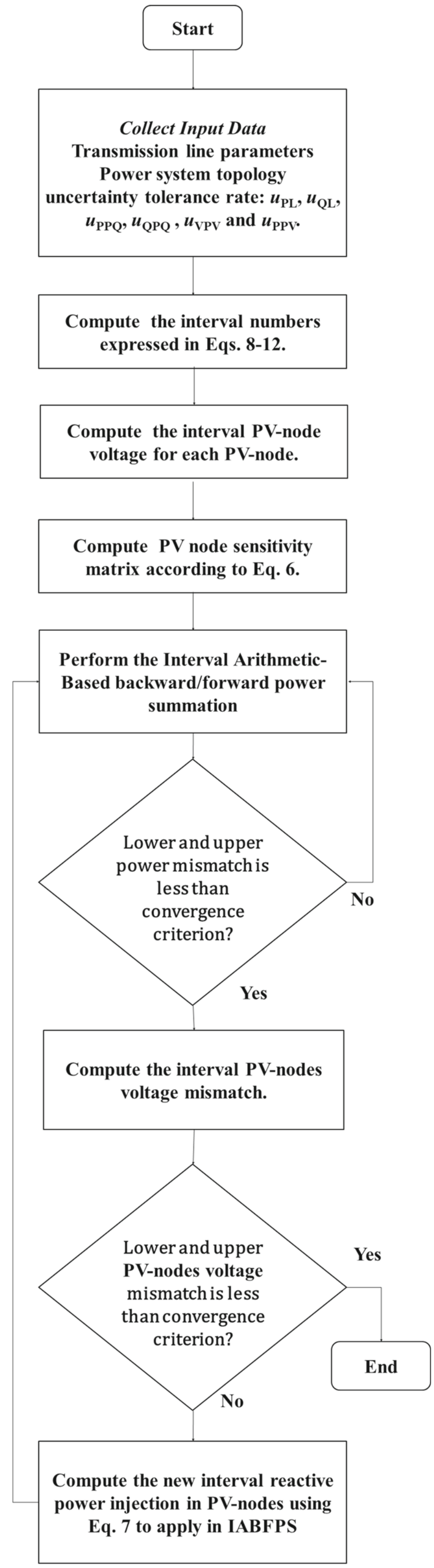

Fig. 1 IABFPS algorithm

4 Application

The proposed algorithm is implemented using MATLAB on a 2 GHz INTEL i7 Quad core personal computer. Three primary distribution systems are selected to illustrate the performance of the proposed algorithm. The test systems

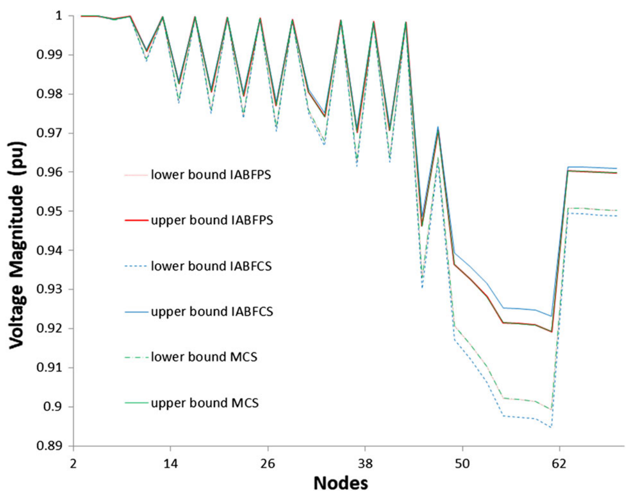

Fig. 2 Bus voltage magnitude bounds with uncertainty tolerance of 10% in the 69-node test system

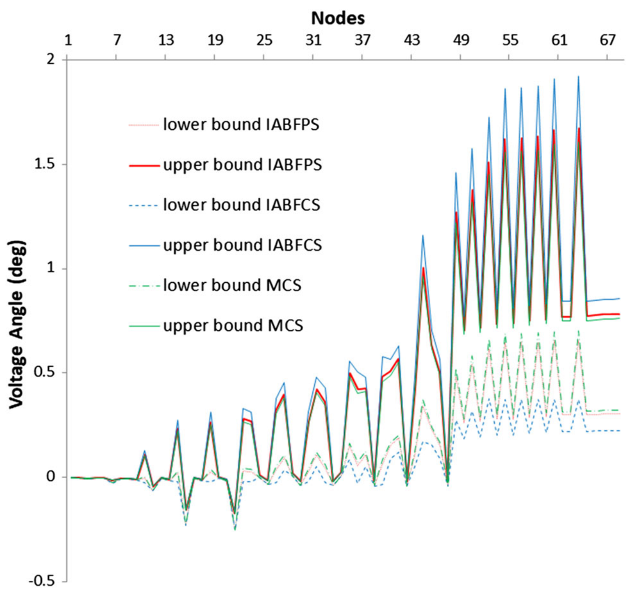

Fig. 3 Bus voltage angle bounds with uncertainty tolerance of 10% in the 69-node test system

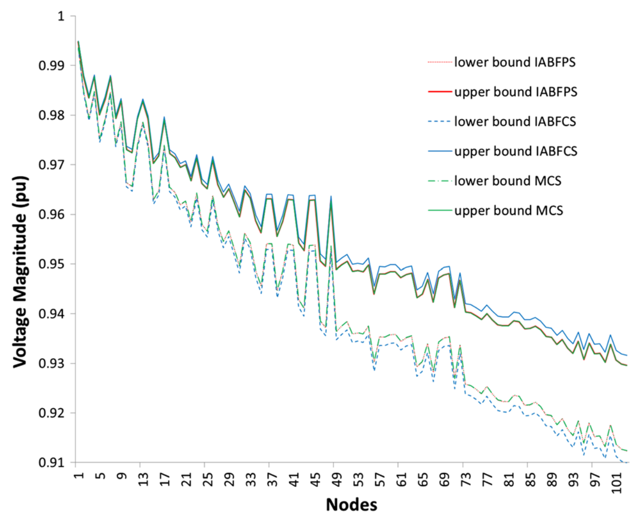

Fig. 4 Bus voltage magnitude bounds with uncertainty tolerance of 30% in the 104-node test system

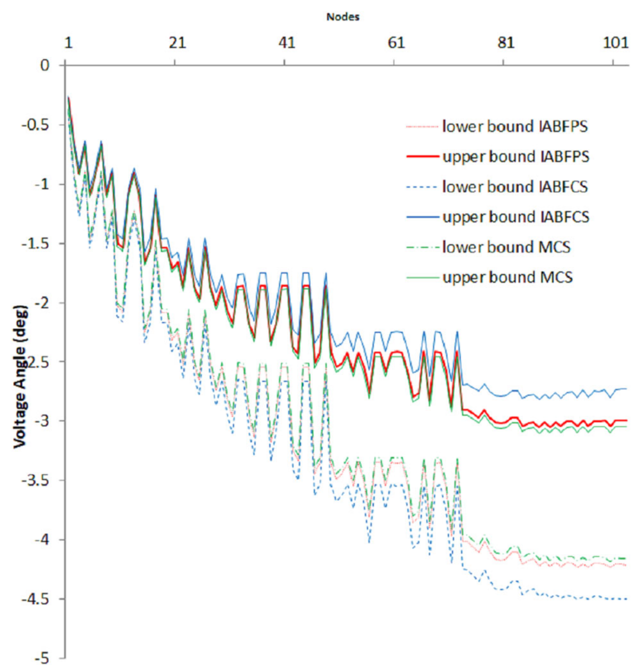

Fig. 5 Bus voltage angle bounds with uncertainty tolerance of 30% in the 104-node test system

are a 69-node radial distribution system with line voltage of 12.66 kV (Das 2002), a 104-node radial distribution system with line voltage of 13.8 kV (Alves et al. 2005) and a 282-node radial distribution system with line voltage of 13.8 kV (Alves and Sousa 2014). None of them have DGs allocated in their original configuration.

In order to illustrate the effectiveness of IABFPS, a MCS is used for comparison. MCS steps are summarized as follows.

1. Consider $X = \mathrm{PL}_k$ and $u_X = u_{\mathrm{PL}}$ (Eq. 8);
2. Generate a random number (RN) using rand function from MATLAB that follow the standard uniform distribution on the open interval (0, 1);
3. If $RN < 0.5$, then signal $= -1$ else signal $= +1$;
4. Generate another random number (RN);
5. Generate random DG output power or random load:

$$Y = X + \text{signal} * X * RN * u_X/100;$$

6. Repeat steps 2–5 for each one of group of variables: $\{X = \mathrm{QL}_k$ and $u_X = u_{\mathrm{QL}}$ (Eq. 9)$\}$, $\{X = \mathrm{PPQ}_k$ and $u_X = u_{\mathrm{PPQ}}$ (Eq. 10)$\}$, $\{X = \mathrm{QPQ}_k$ and $u_X = u_{\mathrm{QPQ}}$ (Eq. 11)$\}$ and $\{X = \mathrm{PPV}_k$ and $u_X = u_{\mathrm{PPV}}$ (Eq. 12)$\}$;

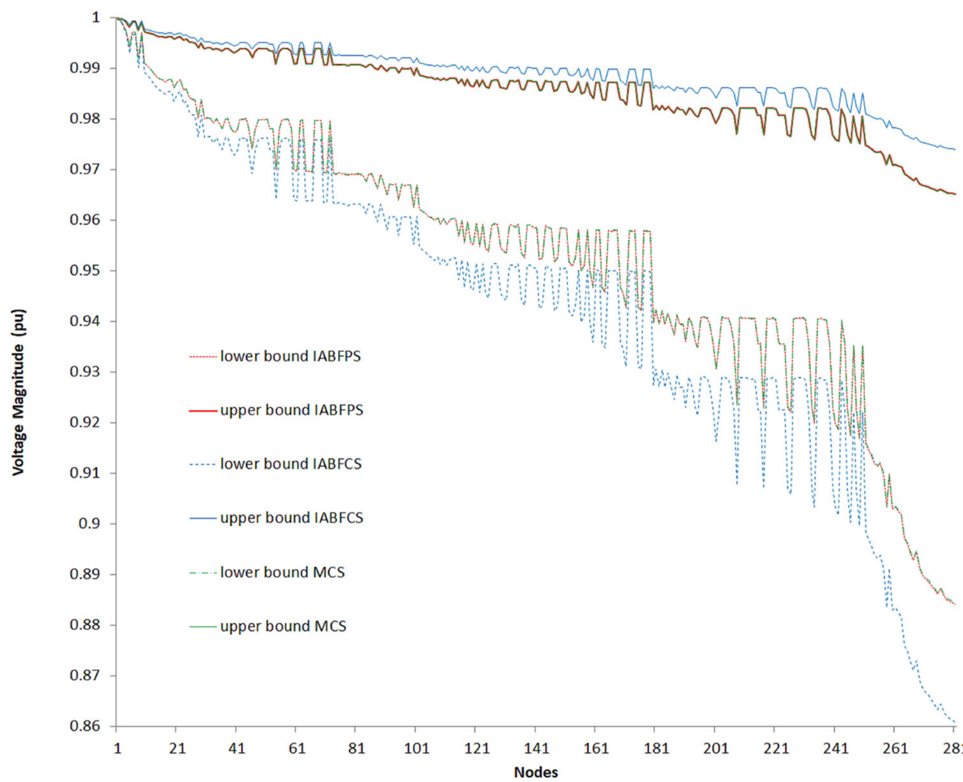

Fig. 6 Bus voltage magnitude bounds with uncertainty tolerance of 50% in the 282-node test system

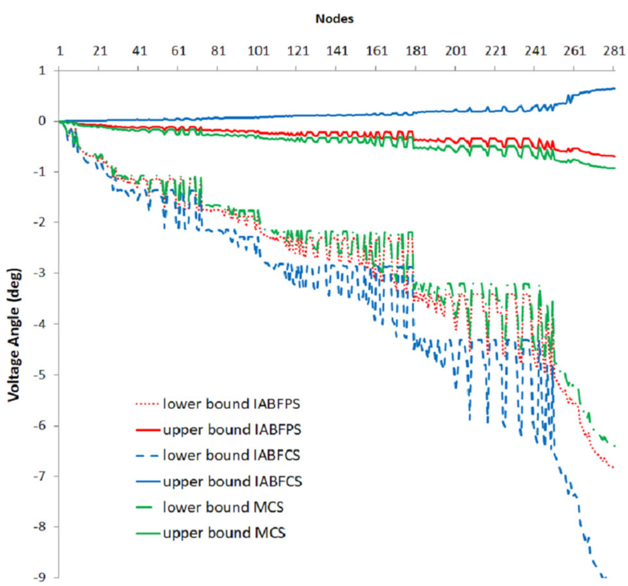

Fig. 7 Bus voltage angle bounds with uncertainty tolerance of 50% in the 282-node test system

7. Run the deterministic BFPS using the DGs output power and loads samples obtained in steps 1–6 to determine a trial for MCS;
8. Repeat steps 1–7 for N times (N is the number of trials generated for MCS).

Table 1 Voltage magnitude error under different uncertainty tolerances

Unc. Tol. (%)	Algorithm	Max. error voltage magnitude (pu)		
		69-node	104-node	282-node
± 10	IABFPS	0.00005	0.00005	0.00003
	IABFCS	0.00469	0.00247	0.00283
± 20	IABFPS	0.00018	0.00013	0.0001
	IABFCS	0.01058	0.00541	0.00637
± 30	IABFPS	0.00017	0.00014	0.00007
	IABFCS	0.01854	0.00921	0.01056
± 40	IABFPS	0.00019	0.0003	0.00022
	IABFCS	0.02934	0.01359	0.01585
± 50	IABFPS	0.0005	0.00029	0.00029
	IABFCS	0.04536	0.01928	0.02352

The lower and upper bounds of MCS are set as the minimum and the maximum values obtained in MCS iterations.

4.1 IABFPS × IABFCS

In order to demonstrate the effectiveness of the proposed algorithm, IABFPS is compared with IABFCS (Das 2002). In Das (2002) is not considered the presence of DGs. A MCS with 100,000 trials by bus system is also produced. It should be noted that increasing the number of MCS beyond 100,000 trials did not yield any significant changes to the solution intervals. The uncertainty tolerance rates for active and reac-

Table 2 Voltage angle error under different uncertainty tolerances

Unc. Tol. (%)	Algorithm	Max. error voltage angle (°)		
		69-node	104-node	282-node
± 10	IABFPS	0.065	0.054	0.066
	IABFCS	0.330	0.344	0.379
± 20	IABFPS	0.146	0.119	0.141
	IABFCS	0.701	0.731	0.816
± 30	IABFPS	0.247	0.188	0.225
	IABFCS	1.143	1.193	1.328
± 40	IABFPS	0.375	0.277	0.324
	IABFCS	1.689	1.719	1.945
± 50	IABFPS	0.518	0.363	0.428
	IABFCS	2.444	2.389	2.810

Table 3 DGs allocated in each bus system

Bus system	Node	DG	*P* (kW)	*Q* (kVAr)	*V* (pu)
69-node	04	PV	800		1.00
	26	PV	5000		1.03
104-node	13	PV	8000		1.02
	38	PQ	600	200	
282-node	07	PQ	500	100	
	242	PV	2600		1.00

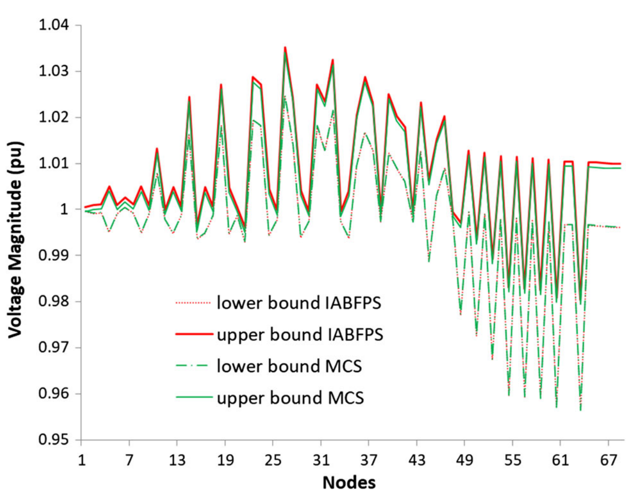

Fig. 8 Bus voltage magnitude bounds with uncertainty tolerance of 10% in the 69-node test system with DGs

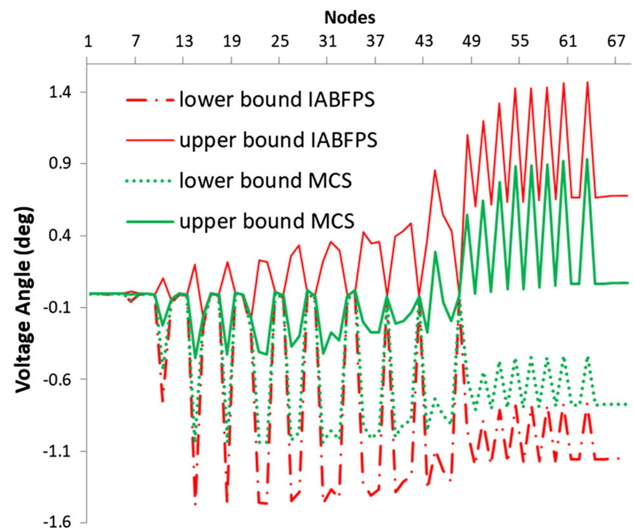

Fig. 9 Bus voltage angle bounds with uncertainty tolerance of 10% in the 69-node test system with DGs

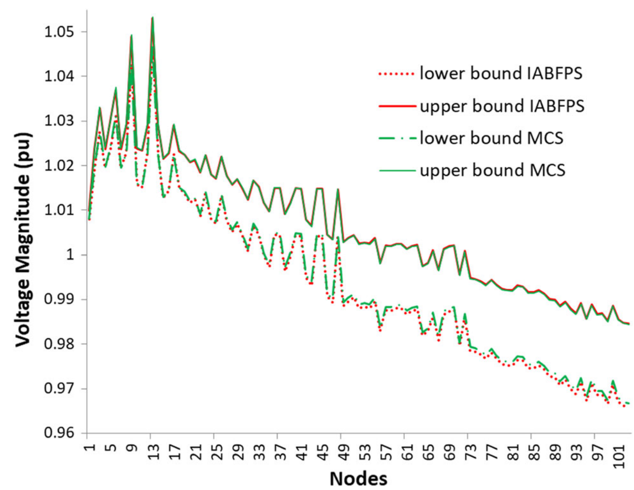

Fig. 10 Bus voltage magnitude bounds with uncertainty tolerance of 30% in the 104-node test system with DGs

tive power of load are assumed varying from 10 to 50%. Due to limitation of space, only some output bounds obtained by the power flow algorithms studied in this paper are represented.

In Figs. 2 and 3 are illustrated the bus voltage magnitude and the bus voltage angle bounds for 69-node distribution system considering the uncertainty tolerance of 10%. In Figs. 4 and 5 are illustrated the bus voltage magnitude and the bus voltage angle bounds for 104-node distribution system considering the uncertainty tolerance of 30%. In Figs. 6 and 7 are illustrated the bus voltage magnitude and angle bounds for 282-node distribution system considering the uncertainty tolerance of 50%. The results are presented in degree for voltage angle and in per-unit system for voltage magnitude.

Considering the Monte Carlo simulation results as reference, Table 1 shows the maximum error of lower and upper voltage magnitude bounds found in IABFPS and IABFCS. Table 2 shows the maximum error of lower and upper voltage angle bounds found in both algorithms.

All those results (Figs. 2, 3, 4, 5, 6 and 7 and Tables 1 and 2) present consistently that the error produced by IABFPS is much less than the error produced by IABFCS. Besides, the results produced by IABFPS are so close to the results pro-

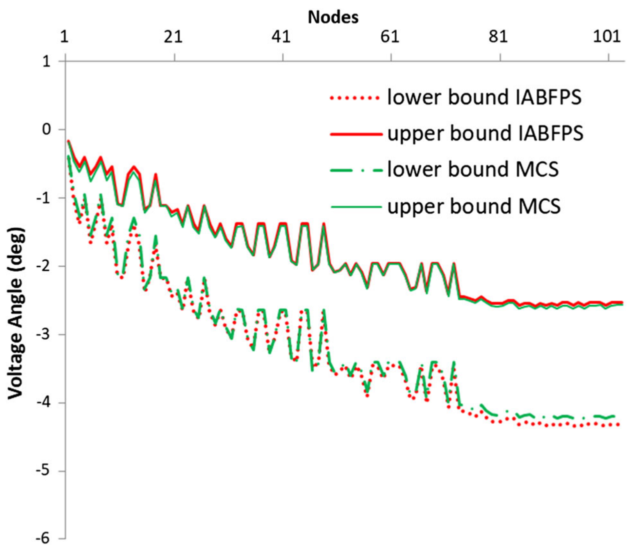

Fig. 11 Bus voltage angle bounds with uncertainty tolerance of 30% in the 104-node test system with DGs

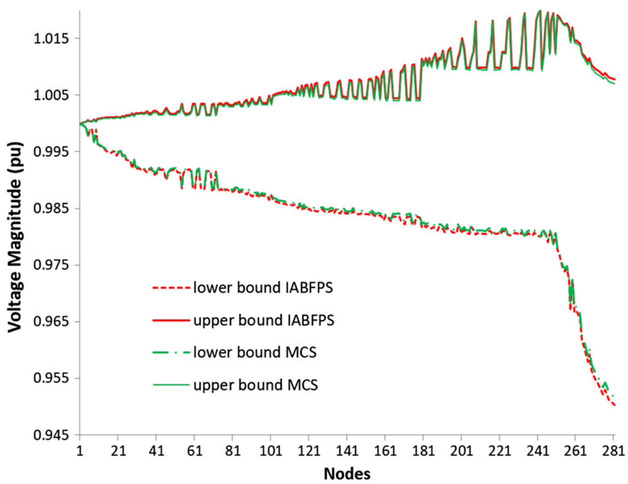

Fig. 12 Bus voltage magnitude bounds with uncertainty tolerance of 50% in the 282-node test system with DGs

duced by MCS. As expected, the ranges of solutions obtained by IABFPS contain the bounds obtained by the Monte Carlo simulation. This overlap demonstrates that IABFPS produces proper approximations of the power flow solution bounds. The number of iterations to converge in both algorithms is similar varying from 5 to 8 iterations. The simulation time required by test systems ranged from 0.13 to 0.22 s.

4.2 IABFPS Considering the Presence of DGs

In order to demonstrate the effectiveness of the proposed algorithm with the presence of DGs, DGs allocated in each test system are considered according to Table 3. DGs units modelled as PV-node and PQ-node are considered.

The allocation and sizing of DGs along the feeder is chosen to ensure the improvement in the voltage profile in each

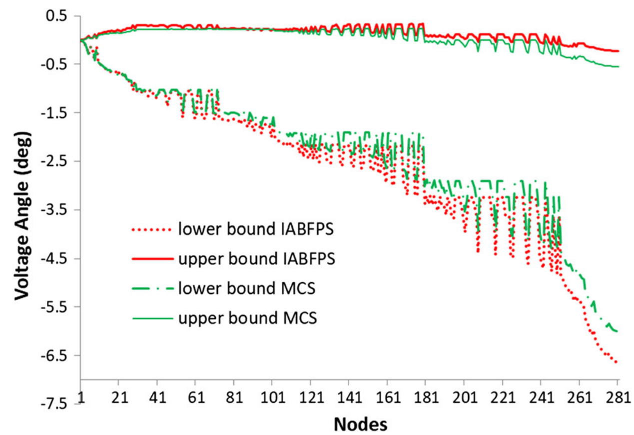

Fig. 13 Bus voltage angle bounds with uncertainty tolerance of 50% in the 282-node test system with DGs

Table 4 Voltage magnitude error analysis under different uncertainty tolerances considering DGs allocation

Uncertainty Tol. (%)	Max. error voltage magnitude (pu)		
	69-node	104-node	282-node
± 10	0.00045	0.00458	0.00263
± 20	0.0017	0.00507	0.00267
± 30	0.00094	0.00842	0.00259
± 40	0.00132	0.01431	0.00284
± 50	0.00995	0.01138	0.00378

Table 5 Voltage angle error analysis under different uncertainty tolerances considering DGs allocation

Uncertainty Tol. (%)	Max. error voltage angle (°)		
	69-node	104-node	282-node
± 10	0.652	0.116	0.238
± 20	0.842	0.176	0.27
± 30	1.274	0.274	0.289
± 40	1.566	0.339	0.465
± 50	1.794	0.647	0.64

test system. In Table 3, P and Q represent the nominal active and reactive power of DGs. The uncertainty tolerance rates for active power of PQ-node DG, reactive power of PQ-node DG and active power of PV-node DG are defined in 20% for all test systems. It is assumed that the uncertainties assigned to output power of DGs (20%) can be provided for each one of them.

The proposed algorithm is compared with a Monte Carlo simulation with 100,000 trials for each bus system. Uncertainty tolerance rate for PV-node voltage is assumed as up to 1% for 69-node system, 0% for 104-node system (not considering uncertainties in PV-node voltage) and up to 2% for 282-node system. Those uncertainty tolerance rates have

Table 6 Interval reactive power of PV-node DG obtained for each bus system

Unc. Tol. (%)	69-node (MVAr)		104-node (MVAr)	282-node (MVAr)
	04	26	13	242
± 10	[+ 0.92, + 1.05]	[− 10.0, − 2.46]	[− 10.6, + 2.57]	[− 3.94, + 0.10]
± 20	[+ 1.14, + 1.19]	[− 10.2, − 2.29]	[− 10.8, + 2.69]	[− 4.09, + 0.24]
± 30	[+ 0.85, + 1.33]	[− 12.0, − 0.65]	[− 11.0, + 2.89]	[− 4.17, + 0.31]
± 40	[+ 0.69, + 1.43]	[− 12.6, − 0.19]	[− 11.2, + 294]	[− 4.42, + 0.53]
± 50	[+ 0.10, + 1.21]	[− 13.2, +0.26]	[− 11.3, + 2.96]	[− 4.60, + 0.68]

been assumed only to assess the effectiveness of the methodology for range defined in the algorithm (uncertainty of up to 2% of the specified voltage value). The uncertainty tolerance rates for active and reactive power of load are assumed varying from 10 to 50%.

In Figs. 8 and 9 are illustrated the bus voltage magnitude and the bus voltage angle bounds for 69-node distribution system considering two PV-node DGs allocated (Table 3) and an uncertainty tolerance of 10%. In Figs. 10 and 11 are illustrated the bus voltage magnitude and the bus voltage angle bounds for 104-node distribution system considering a PV-node and a PQ-node DG allocated (Table 3) and an uncertainty tolerance of 30%. In Figs. 12 and 13 are illustrated the bus voltage magnitude and the bus voltage angle bounds for 282-node distribution system considering a PV-node and a PQ-node DG allocated (Table 3) and an uncertainty tolerance of 50%.

Considering the Monte Carlo simulation results as reference, Tables 4 and 5, respectively, show the maximum error of lower and upper voltage magnitude and angle bounds found in IABFPS.

As expected, in Tables 4 and 5 are shown that the larger the uncertainty tolerance for load demands, the larger are the maximum errors. Comparing Tables 1 and 2 with Tables 4 and 5, verify that the maximum errors increase with the presence of DGs. Nevertheless, the results produced by IABFPS are still close to the results produced by MCS. The number of iterations for IABFPS convergence varied from 8 to 20 iterations. The simulation time required by test systems ranged from 0.65 to 0.82 s. In Table 6 is shown the interval reactive power of PV-node DG obtained for each bus system.

All results presented in this section confirm that IABFPS achieves proper approximations of the power flow solution bounds.

5 Conclusions

This study presented an interval arithmetic-based power flow algorithm for radial distribution network using backward/forward power summation method. Distributed generation was considered. This algorithm is applied to consider the uncertainties in distributed generation and loads. The main stages and characteristics of IABFPS algorithm and its application in the proposed problem were described. In order to illustrate the performance of the algorithm, several experiments using three test systems were conducted. Proposed algorithm produced better results as compared with an algorithm presented in the literature based on backward/forward current summation method. The results produced by IABFPS were so close to the results produced by a Monte Carlo simulation. The computational performance of proposed algorithm was very fast (milliseconds) even considering the presence of DGs. IABFPS algorithm demonstrated complete adaptation, producing proper results when PV-node DGs were considered. The proposed algorithm has shown a great potential to assist in planning of distribution networks and also to make improvements in existing networks considering uncertainties in distributed generation and loads.

Future work will be focused on investigating the affine arithmetic-based algorithm as tool to assess the uncertainties. Considering the increasing level of wind energy penetration into the grid, uncertainties of the active power produced by wind turbine generating system will be also considered.

References

Alvarado, F. L., Hu, Y., & Adapa, R. (1992). Uncertainty in power system modeling and computation. *Proceedings of IEEE International Conferen Systems, Man and Cybernetics, 1,* 754–760.

Alves, H. N., & Sousa, R. S. (2014). A multi-population genetic algorithm to solve multi-objective remote switches allocation problem in distribution networks. In *2014 IEEE symposium on proceedings of computational intelligence for engineering solutions* (CIES) (pp. 155–164).

Alves, H. N., Souza, B. A., & Ferreira, H. A. (2005). Banks of automatic capacitors in electrical distribution systems: A hibrid algorithm of control. *Rev. Cont. & Automação, 16*(1), 93–99.

Bijwe, P. R., Hanmandlu, M., & Pande, V. N. (2005). Fuzzy power flow solutions with reactive limits and multiple uncertainties. *Electric Power Systems Research, 76,* 145–152.

Borkowska, B. (1974). Probabilistic load flow. *IEEE Transactions on Power Apparatus and Systems PAS, 93*(6), 752–755.

Cheng, C. S., & Shirmohammadi, D. (1995). A three-phase power flow method for real-time distribution system analysis. *IEEE Transactions on Power Systems, 10,* 671–679.

Das, B. (2002). Radial distribution system power flow using interval arithmetic. *International Journal of Electrical Power & Energy Systems, 24*(10), 827–836.

Das, B. (2014). Uncertainty modeling of wind turbine generating system in power flow analysis of radial distribution network. *Electric Power Systems Research, 111,* 141–147.

Das, D., Nagi, H. S., & Kothari, D. P. (1994). Novel method for solving radial distribution network. *IEE Proceedings Generation, Transmission and Distribution, 141*(4), 291–298.

Gu, W., Luo, L., Ding, T., Meng, X., & Sheng, W. (2014). An affine arithmetic-based algorithm for radial distribution system power flow with uncertainties. *International Journal of Electrical Power & Energy Systems, 58,* 242–245.

Hadjsaid, N., Canard, J. F., & Dumas, F. (1999). Dispersed generation impact on distribution networks. *IEEE Computer Applications in Power, 12*(2), 22–28.

Kenarangui, R., & Seifi, A. (1994). Fuzzy power flow analysis. *Electric Power Systems Research, 29,* 105–109.

Li, W. (2005). *Risk assessment of power systems: Models, methods, and applications*. New York: IEEE Press.

Liao, X., Liu, K., Zhang, Y., Wang, K., & Qing, L. (2017). Interval method for uncertain power flow analysis based on Taylor inclusion function. *IET Generation, Transmission and Distribution, 11*(5), 1270–1278.

Luo, L., Gu, W., Wang, Y., & Chen, C. (2017). An affine arithmetic-based power flow algorithm considering the regional control of unscheduled power fluctuation. *Energies, 10,* 1794.

Pereira, L. E. S., Da Costa, V. M., & Rosa, A. L. S. (2012). Interval arithmetic in current injection power flow analysis. *International Journal of Electrical Power & Energy Systems, 43*(1), 1106–1113.

Su, C. L. (2005). Probabilistic load flow computation using point estimate method. *IEEE Transactions on Power Systems, 20,* 1843–1851.

Vaccaro, A., Canizares, C., & Villacci, D. (2010). An affine arithmetic-based methodology for reliable power flow analysis in the presence of data uncertainty. *IEEE Transactions on Power Systems, 25*(2), 624–632.

Vaccaro, A., & Villacci, D. (2009). Radial power flow tolerance analysis by interval constraint propagation. *IEEE Transactions on Power Systems, 24*(1), 28–39.

Wang, S., Wang, K., Teng, F., Strbac, G., & Wu, L. (2018). An affine arithmetic-based multi-objective optimization method for energy storage systems operating in active distribution networks with uncertainties. *Applied Energy, 223,* 215–228.

Zhang, C., Chen, H., Hgan, H., Yang, P., & Hua, D. (2017). A mixed interval power flow analysis under rectangular and polar coordinate system. *IEEE Transactions on Power Systems, 32*(2), 1422–1429.